Anomalous thermoelectric power of the $Mg_{1-x}Al_xB_2$ system with $x = 0.0–1.0$

2008 J. Phys.: Condens. Matter 20 095205

(http://iopscience.iop.org/0953-8984/20/9/095205)

J. Phys.: Condens. Matter **20** (2008) 095205 (6pp) doi:10.1088/0953-8984/20/9/095205

Anomalous thermoelectric power of the $Mg_{1-x}Al_xB_2$ system with $x = 0.0$–1.0

Monika Mudgel[1], V P S Awana[1,4], R Lal[1], H Kishan[1], L S Sharth Chandra[2], V Ganesan[2], A V Narlikar[2] and G L Bhalla[3]

[1] Superconductivity and Cryogenics Division, National Physical Laboratory, Dr K S Krishnan Marg, New Delhi-110012, India
[2] UGC-DAE Consortium for Scientific Research, University Campus, Khandwa Road, Indore-452017, India
[3] Department of Physics and Astrophysics, University of Delhi, Delhi-110007, India

E-mail: awana@mail.nplindia.ernet.in

Received 13 November 2007, in final form 14 January 2008
Published 8 February 2008
Online at stacks.iop.org/JPhysCM/20/095205

Abstract

The thermoelectric power, $S(T)$, of the $Mg_{1-x}Al_xB_2$ system has been measured for $x = 0.0$, 0.1, 0.2, 0.4, 0.6, 0.8 and 1.0. X-ray diffraction, resistivity and magnetization measurements are also presented. It has been found that the thermoelectric power is positive for $x \leqslant 0.4$ and is negative for $x \geqslant 0.6$ over the entire temperature range studied up to 300 K. The thermoelectric power of $x \leqslant 0.4$ samples vanishes discontinuously below a certain temperature, implying the existence of superconductivity. In general, the magnitude of the thermoelectric power increases with temperature up to a certain temperature, and then it starts to decrease towards a zero baseline. In order to explain the observed behavior of the thermoelectric power, we have used a model in which diffusion and phonon drag processes are combined, by using a phenomenological interpolation between the low and high temperature behaviors of the thermoelectric power. The model considered provides an excellent fit to the observed data. It is further found that Al doping enhances the Debye temperature.

(Some figures in this article are in colour only in the electronic version)

1. Introduction

With the advent of high temperature superconductivity in 1986 [1] the possibility of electron–phonon interaction as a superconductivity mechanism seemed low. However, the situation changed after the discovery of superconductivity at 39 K in MgB_2 [2], when it was realized that the mechanism of superconductivity could yet be based on the electron–phonon interaction within the strong coupling limits [3]. This was perceived from the fact that, both Mg and B being light elements, their lattice contributions could be sufficiently strong to promote the relatively high T_c observed [4]. Besides, the lattice of MgB_2 is stretched in the c-direction in comparison to those of other same structure borides, namely, TaB_2, AlB_2, ZrB_2 and MoB_2 [5–7]. A stretched lattice may result in instability and hence further contribution to phonon interactions. It seems that the basic stretched lattice structure of MgB_2 being constructed from relatively light elements Mg and B is responsible for the strong electron–phonon interaction. MgB_2 possess simple hexagonal AlB_2-type structure with space group P_6/mmm. It contains graphite-type boron layers, which are separated by hexagonal close-packed layers of magnesium. The magnesium atoms are located at the centers of hexagons formed of boron. The spacing between the boron planes is significantly larger than the in-plane B–B spacing. In fact, the characteristic c/a ratio is $\sim$1.14 in MgB_2, while it is $\sim$1.08 in AlB_2.

Another important difference between MgB_2 and AlB_2 is that in MgB_2 the cation (Mg^{2+}) is divalent while in AlB_2 the cation (Al^{3+}) is trivalent. This means that if we gradually replace Mg by Al, the population of the holes in the two-dimensional (2D) σ-band will start decreasing. In fact, it has been shown using band structure calculations that the σ-band is placed lower than the Fermi energy in AlB_2 [3, 8]. So substitution of Mg by Al will fill the σ-band completely

[4] Author to whom any correspondence should be addressed www.freewebs.com/vpsawana/.

(with electrons) even before a 100% substitution level. In this situation, only the π-band will take part in various physical processes so the system will no longer be a two-band (σ-band and π-band) system. This two-band to one-band system crossover with increasing substitution of Mg by Al in MgB_2 prompted us to carry out the present study of the $Mg_{1-x}Al_xB_2$ system for $x = 0.0$ to 1.0. Earlier reports on $Mg_{1-x}Al_xB_2$ were limited to $x \leqslant 0.4$ [5], $x \leqslant 0.1$ [9] and $x \leqslant 0.5$ [10] only. Slusky *et al* [5] have studied the crystal structure and magnetization of $Mg_{1-x}Al_xB_2$ for $x \leqslant 0.4$. Their main finding is that Al doping near 10% causes partial collapse of the spacing between boron layers and that the superconductivity has a close connection with such a structural instability. Lorenz *et al* [9] have measured the thermoelectric power (TEP) of the Al-substituted samples up to $x = 0.1$. They made an effort to explain the observed behavior of the TEP on the basis of the *parabolic one-band model*. Very recently, Monika *et al* [10] have presented a detailed x-ray diffraction study along with resistivity and magnetization measurements for the $Mg_{1-x}Al_xB_2$ for $x \leqslant 0.5$. Mainly, the existence of superstructure is shown in the $Mg_{0.5}Al_{0.5}B_2$ system.

In this paper we focus on the thermoelectric power of $Mg_{1-x}Al_xB_2$ for Al concentrations ranging from $x = 0.0$ to 1.0. This wide range of x values allows us to study the behavior of the $Mg_{1-x}Al_xB_2$ system for varying contributions of the σ-band. Recently Souma and Takahashi [11] (cf figures 1 and 4 of this reference) had shown the π-band structure to be essentially same for MgB_2 and AlB_2. So, we can consider the contributions of the π-band to be similar for all x. As mentioned above, the TEP of $Mg_{1-x}Al_xB_2$ was observed earlier also [9], but for $x \leqslant 0.1$. We shall not only present TEP data for $Mg_{1-x}Al_xB_2$ for a much wider range of x ($0.0 \leqslant x \leqslant 1.0$) but we shall also provide a reasonable explanation of the TEP behavior. In fact the explanation of the TEP behavior given by Lorenz *et al* [9] for the $Mg_{1-x}Al_xB_2$ system and also by Gahtori *et al* for the $Mg_{1-x}Fe_xB_2$ system [12] seems defective for the following reasons. (1) The linear theoretical fits based on the parabolic one-band model used by these authors do not pass through the origin of the temperature–TEP plane. This amounts to inconsistency because according to equation (3) of Lorenz *et al* and equation (12) of Gahtori *et al* [12], the TEP should vanish for zero temperature. On the other hand, Lorenz *et al* find $S = -1.0\ \mu V\ K^{-1}$ for $T = 0$, and Gahtori *et al* find $S = -1.2\ \mu V\ K^{-1}$ for $T = 0$ for their respective MgB_2 samples. (Here S denotes the TEP and T denotes the temperature.) These values are quite significant as the TEP of MgB_2 is of the order of $1.0\ \mu V\ K^{-1}$ (near 50 K) for both cases. (2) The agreement between the theoretical model and experimental results tends to become poorer with increasing temperature within the one-band model employed by Lorenz *et al* and Gahtori *et al* (cf figure 2 of [9] and figure 3 of [12]). For a realistic explanation of the TEP, we, in the present paper, shall consider the phonon drag contribution also. Apart from this, we shall also consider the high T behavior of the TEP simultaneously.

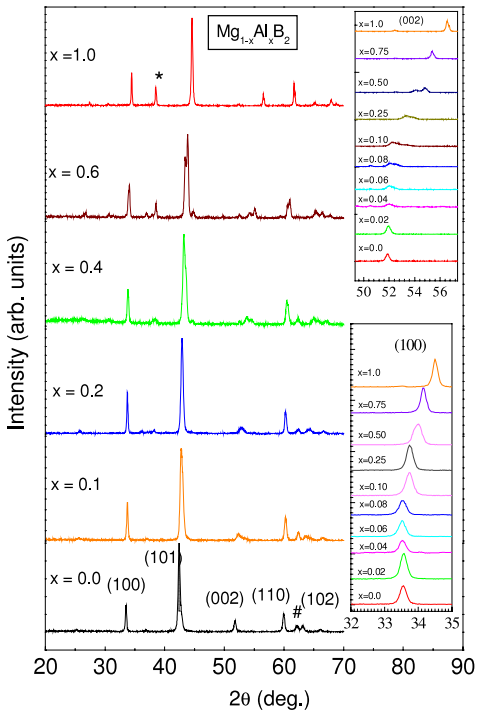

Figure 1. XRD patterns for the $Mg_{1-x}Al_xB_2$ series ($x = 0.0$ to 1.0). Upper and lower insets show shifts of the (002) and (100) peaks, respectively.

2. Experimental details

Polycrystalline $Mg_{1-x}Al_xB_2$ samples with $x = 0.0$, 0.10, 0.20, 0.40, 0.60, 0.80 and 1.0 are synthesized by the solid-state reaction route with ingredients Mg, B, and Al. The Mg powder used is from Reidel-de-Haen of assay 99%. The B powder is amorphous, and of Fluka make of assay 95–97%. The Al powder is from Reidel-de-Haen with above 93% assay. For synthesis of $Mg_{1-x}Al_xB_2$ samples, the nominal weighed samples are ground thoroughly, pelletized, encapsulated in soft iron tubes and put in a programmable furnace under a flow of argon at one atmosphere pressure. The temperature of the furnace is programmed to reach 850 °C over 2 h, held at the same temperature for two and a half hours, and subsequently cooled to room temperature over a span of 6 h in the same argon atmosphere. X-ray diffraction patterns were taken using Ni filtered Cu Kα radiation. Resistivity measurements were carried out by the conventional four-probe method. Thermoelectric power measurements were carried out by the dc differential technique over a temperature range of 5–300 K, using a home made set-up. A temperature gradient of $\sim$1 K was maintained throughout the TEP measurements. Magnetization measurements are carried out with a Quantum-Design SQUID magnetometer MPMS-7.

3. Results and discussion

Room temperature x-ray diffraction (XRD) patterns for the $Mg_{1-x}Al_xB_2$ with $x = 0.0$–1.0 are shown in figure 1. All the samples crystallize in simple hexagonal AlB_2-type

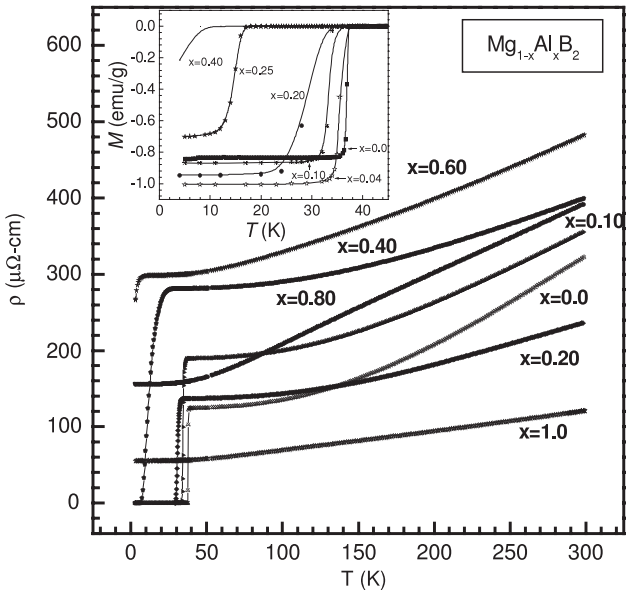

Figure 2. Resistivity versus temperature plots for all $Mg_{1-x}Al_xB_2$ samples ($x = 0.0$ to 1.0). The inset shows the zero-field cooled (ZFC) magnetization as a function of temperature for superconducting $Mg_{1-x}Al_xB_2$ ($x = 0.0$ to 0.40) samples.

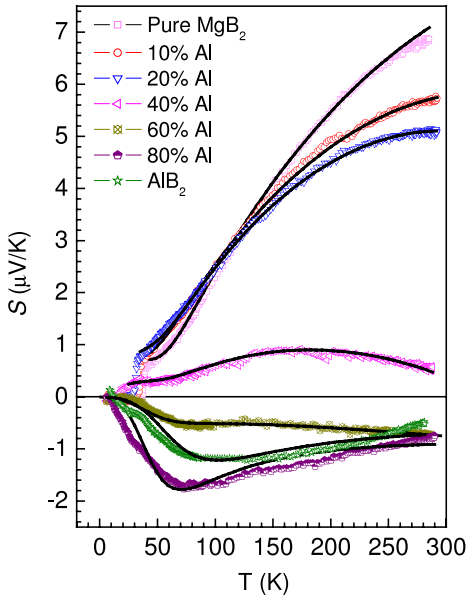

Figure 3. Thermopower versus temperature plots in the temperature range 0–300 K for all samples of the series $Mg_{1-x}Al_xB_2$ ($x = 0.0$ to 1.0). The experimental data points are shown by different symbols, while the theoretical fits to equation (7) are shown by solid lines.

structure with space group P_6/mmm. For a pristine sample all characteristic peaks are indexed and are well corroborated with the literature [2, 4, 5, 10]. With successive substitution of Al at Mg sites in $Mg_{1-x}Al_xB_2$, up to $x = 0.40$, although the structure (hexagonal) and space group P_6/mmm remain the same, all the XRD peak positions are shifted towards the higher angle side, indicating a decrease in lattice parameters. The upper and lower insets of figure 1 show shifts of (002) and (100) peaks confirming the decreases of the a and c parameters. For MgB_2, $a = 3.0857$ Å and $c = 3.5230$ Å, while for AlB_2, $a = 3.0036$ Å and $c = 3.2519$ Å. For other samples of the series both a and c lattice parameters have intermediate values according to the Al content in them. The structural anomaly related to broadening of the (002) peak up to $x = 0.50$ is described in detail by us elsewhere [10]. Here we have analyzed the samples up to full Al substitution. Beyond $x = 0.50$, some additional phases arise, as shown by $*$ in figure 1, which might be due to AlB_4.

Resistivity versus temperature plots of the $Mg_{1-x}Al_xB_2$ series with $x = 0.0$, 0.10, 0.20, 0.40, 0.60, 0.80 and 1.0 are shown in figure 2. In the normal state, i.e. above T_c, all samples show metallic behavior. The normal state ρ–T plot of our pure MgB_2 corresponds to $\rho(300)/\rho(T_c) \sim 3$, which agrees with that for the MgB_2 samples of Lorenz *et al* [9] and Gahtori *et al* [12]. The critical temperature $T_c(\rho = 0)$ for pristine samples is about 38 K. As we substitute Al, loss of superconductivity is observed in terms of decreasing critical temperatures [9, 13, 14]. In fact T_c is 34, 30 and 7 K for Al contents of 10%, 20% and 40% respectively. This means that there is a slow decrease in T_c up to $x = 0.20$, which is followed by a much sharper decrement up to $x = 0.40$. The samples are no longer superconducting ($\rho = 0$) beyond $x = 0.40$, while the sample with $x = 0.60$ exhibits a T_c^{onset} only. The superconducting transition width is small up to $x = 0.20$ samples, but for the $x = 0.40$ sample, T_c^{onset} is 26.2 K, while T_c ($\rho = 0$) is only 6.9 K. No superconductivity (in terms of $\rho = 0$) is observed in $Mg_{0.5}Al_{0.5}B_2$ samples, and beyond that magnetization measurements (χ–T) for the $Mg_{1-x}Al_xB_2$ series with $x = 0.0$, 0.04, 0.10, 0.20, 0.25 and 0.40 are shown in the inset of figure 2. The critical temperatures obtained from this (T_c^{dia}) are in close agreement with the critical temperature ($T_c^{\rho=0}$) obtained from resistivity measurements except in the case of $x = 0.40$ for which a broad transition is seen and the saturation of moment is not seen down to 5 K. Qualitatively, ρ–T and χ–T measurements confirm similar decreases in T_c with Al doping. The decrease of T_c with Al can easily be explained in terms of electron doping. Each Al atom provides an extra electron and results in hole band filling. Electron doping raises the Fermi level to higher energies and hence the density of states decreases at the Fermi level, which results in loss of superconductivity. It is believed that the superconductivity in $Mg_{1-x}Al_xB_2$ is due to electron–phonon interaction, and that the T_c suppression due to increasing Al is caused by the lowering of the σ-band [8]. Moreover, lattice parameters also decrease continuously with Al doping. The c/a value for MgB_2 is 1.14 while it is just 1.08 for AlB_2. So the AlB_2 lattice is quite compressed in comparison to MgB_2. This lattice strain also affects the electron–phonon interactions and hence may be a secondary reason for the suppression of superconductivity.

The measured thermoelectric powers of the $Mg_{1-x}Al_xB_2$ samples for $x = 0.0$, 0.1, 0.2, 0.4, 0.6, 0.8 and 1.0 are presented in figure 3 by using different symbols for different samples. For low x, i.e., $x < 0.4$, the behavior of the TEP is similar to that of the $Mg_{1-x}Al_xB_2$ samples of Lorenz *et al* [9], and to that of the $Mg_{1-x}Fe_xB_2$ samples of Gahtori *et al* [12].

In particular, there is a signature of superconductivity in the behavior of the TEP for the $x \leqslant 0.4$ samples. This is consistent with the magnetization and resistivity measurements shown in figure 2. The TEP of the $x \geqslant 0.6$ samples is negative for all the temperature values considered, signifying the ineffectiveness of the hole based σ-band. Also the TEP of the $x \geqslant 0.6$ samples does not show any feature of superconductivity.

In order to explain the observed behavior of the TEP for the present $Mg_{1-x}Al_xB_2$ samples, we notice that in general this system involves two bands—the σ-band and the π-band. It is believed that the σ-band is primarily responsible for the occurrence of the superconductivity [8]. Then, since the observed behavior of the TEP involves the effect of superconductivity (for $x \leqslant 0.4$), we may say that σ-band holes provide essential contributions to the TEP values in this doping range. Since, for higher x, the extra electrons donated by Al tend to make the σ-band ineffective beyond a certain doping level of Al, it may be argued that the TEP of the $x > 0.4$ samples will arise due to the π-band only. The features of the π-band are reported similar in MgB_2 and AlB_2 [11]; this we will use below for setting a reasonable expression of the TEP.

Theoretically, two processes contribute to the TEP. The first is the diffusion process, and the second is the phonon drag process. The contribution to the TEP due to diffusion process is given by the Mott formula [15]

$$S_d = (\pi^2 k_B^2 T/3e)|[\partial \ln \sigma(\omega)/\partial\omega]|E_F. \quad (1)$$

Here k_B is the Boltzmann constant, e is the carrier charge, $\sigma(\omega)$ is the conductivity corresponding to the electron energy ω, and E_F is the Fermi energy. In the low temperature limit, the carrier relaxation time is limited by impurity scattering. From the extrapolation of the resistivity of $Mg_{1-x}Al_xB_2$ (shown in figure 2) to zero temperature, it turns out that the present samples correspond to significant resistivity at zero temperature. This means that there is an essential presence of impurity scattering in the present samples. Thus for low temperatures, where phonons have not yet started to play a significant role, we can use the conductivity formula [16]

$$\sigma = ne^2\tau/m. \quad (2)$$

Here n is carrier density, τ is carrier relaxation time and m is carrier mass. For a three-dimensional system, it is well known that equations (1) and (2) lead to equation (3) below [15]:

$$S_d = \pi^2 k_B^2 T/3eE_F. \quad (3)$$

In order to obtain an expression for diffusion thermoelectric power corresponding to a two-dimensional band, we follow the same steps as were used in arriving at equation (3) from equations (1) and (2). We use the 2D form of σ from equation (2c) of Fukuyama [16] and find that formally equation (3) is valid for the 2D band also. We emphasize that this is only for parabolic 2D and 3D bands. The result may be different for other band structures. Since the TEP is additive (cf equation H8 of Bailyn [17]), the combined contribution of the 3D π-band and 2D σ-band of the $Mg_{1-x}Al_xB_2$ to the TEP may be written as

$$S_d = (\pi^2 k_B^2 T/3|e|)(W_\sigma^{-1} - W_\pi^{-1}) = AT. \quad (4)$$

Here W_σ is the separation of the Fermi level from the bottom of the hole-like σ-band, and W_π is the separation of the Fermi level from the bottom of the π-band. A is a constant, independent of temperature. From the band structure calculations of An and Pickett [8], one finds that $W_\sigma = 0.72$ eV, and $W_\pi = 7.4$ eV. This means that the contribution of the π-band electrons to S_d is about 10 times smaller than that of the σ-band holes.

As mentioned in the introduction, the diffusion contribution to the TEP leads to an inconsistent explanation of the reported data [9, 12]. In fact, we obtain that the TEP is approximately equal to $-1.0\ \mu V\,K^{-1}$ for $T = 0$, while it should have vanished according to equation (4) used in [9] and [12]. Since equation (4) is justified for $T \to 0$, and also we get inconsistency by the use of equation (4), it becomes necessary to consider the phonon drag contribution along with the diffusion term to the thermoelectric power. For the 3D π-band the phonon drag contribution will vary like T^3 for low T [18], and like T^{-1} for high T [19]. Though for the intermediate temperature values, the behavior of the phonon drag TEP is given by a very complicated expression [17, 19], still it varies smoothly from low T values to the high T values. We thus hope that a simple interpolation will provide a reasonable phenomenology of the variation of the phonon drag contribution to the TEP from $T \to 0$ to $T \to \infty$. Since the TEP varies as T^3 for $T \to 0$ and as T^{-1} for $T \to \infty$, we consider the interpolation

$$S_{pd,\pi} = T^3/(B + CT^4) \quad (5)$$

for the 3D π-band. Here the suffix 'pd' on S implies phonon drag and the suffix 'π' implies the 3D π-band.

From equation (5), we see that $S_{pd,\pi} \to T^3/B$ for $T \to 0$. Here B should vary like θ_D^3 [18].

Here θ_D is the Debye temperature. C is also a constant, but not dependent on θ_D.

In order to work out an expression for the phonon drag contribution of the 2D σ-band, we notice that the 2D character of the σ-band will allow the phonons to drag only in a 2D plane. As a result of this, the feature that led to a T^3 variation of the phonon drag contribution from a 3D band, will lead to a T^2 variation for a 2D band. Thus using an interpolation similar to that of equation (5), we may express the phonon drag TEP due to the σ-band by

$$S_{pd,\sigma} = T^2/(D + ET^3). \quad (6)$$

Notice that here D is expected to vary like θ_D^2. However, since the σ-band changes with Al doping in MgB_2, D may also have a dependence on the electronic structure. We shall see below what the present data inform us of in this connection.

Combining all the contributions from equations (4)–(6), we obtain finally the following expression for the TEP of the $Mg_{1-x}Al_xB_2$ samples:

$$S = AT + T^3/(B + CT^4) + T^2/(D + ET^3). \quad (7)$$

We emphasize that we have not included high T contribution in equation (7) due to the diffusion process. The reason for this is that for higher values of temperature, the

Table 1. Values of the parameters A, B, C and D of equation (7) for various values of the Al content in $Mg_{1-x}Al_xB_2$. The values of E turn out to be less than 10^{-40} so it has been taken as zero for all x in $Mg_{1-x}Al_xB_2$. The relative values of the Debye temperature θ_D/θ_{Do} are also given. θ_D is the Debye temperature of the $x = 0$ sample.

x	A (μV K^{-2})	B (K^4 μV^{-1})	C (μV^{-1})	D (K^3 μV^{-1})	$\theta_D(x)/\theta_{D0}$
0.0	0.040	-5.91×10^4	-8.59×10^{-3}	-2.16×10^4	1.00
0.1	0.036	-6.84×10^4	-17.18×10^{-3}	-1.82×10^4	1.05
0.2	0.036	-10.29×10^4	-17.44×10^{-3}	-1.59×10^4	1.20
0.4	0.012	-37.56×10^4	-38.37×10^{-3}	-2.83×10^4	1.85
0.6	-0.002	-27.97×10^4	-31.11×10^{-3}	—	1.68
0.8	-0.001	-4.89×10^4	-6.43×10^{-3}	—	0.94
1.0	0.0	-21.83×10^4	-6.50×10^{-3}	—	1.55

carrier conductivity will depend upon the electron–phonon interaction [12]. In fact, the conductivity due to the electron–phonon interaction is a complicated expression [12]. We have to take the logarithm of this expression (cf equation (1)), and then perform a differentiation. This is an almost impractical task. So here we have not considered the effect of the electron–phonon interaction on the diffusion of the carriers.

We now turn to the explanation of the observed TEP data. Using equation (7) we have fitted the observed data. The fitting parameters are presented in table 1. The parameter E acquires a practically zero value. From figure 3 we see that equation (7) provides an excellent agreement of the theoretical equation (7) with the observed data over the whole temperature range except for the $x = 0.8$ and 1.0 samples. In fact, the $x = 0.8$ and 1.0 samples also show good agreement qualitatively. In view of such an agreement we would like to know about the relative contributions of the diffusion process and phonon drag process. For this purpose, we take a specific temperature $T = 100$ K, and consider values of S for the $x = 0$ and 0.6 samples. From the calculated values, it turns out that the $x = 0$ sample corresponds to $S_d = 4.0\ \mu$V K^{-1}, $S_{pd,\sigma} = -0.46\ \mu$V K^{-1} and $S_{pd,\pi} = -1.09\ \mu$V K^{-1}. We see that the phonon drag corresponds to a significant contribution. Here we would like to clarify that depending upon the electronic structure, the contribution of the phonon drag process to the TEP may be positive or negative irrespective of the charge of the carriers. This argument is based on the work of Bailyn [20].

We now consider the relative contributions of the diffusion process and phonon drag process to the TEP for the $x = 0.06$ sample at $T = 100$ K. We find $S_d = -0.17\ \mu$V K^{-1}, $S_{pd,\sigma} = 0\ \mu$V K^{-1} and $S_{pd,\pi} = -0.29\ \mu$V K^{-1}. From these values it is clear that the phonon drag process is a dominating process for the TEP contribution in the $x = 0.6$ sample. In fact, as is clear from the values of A of table 1, the diffusion contribution is almost negligible for the $x \geqslant 0.6$ samples. The main reason for this is the very large values of W_π (see above).

In order to extract more information from the parameters of table 1, we first of all notice that the values of the parameter A are significant only for the superconducting ($x \leqslant 0.4$) samples. Moreover, the value of A decreases with increasing x. This is in contradiction with the finding of Lorenz *et al* [9] who obtain an increasing linear-in-T slope of the TEP. An obvious reason for this is the modification of the theoretical TEP due to phonon drag. In fact, Lorenz *et al* have not considered phonon drag. In order to see how phonon drag may affect the value of the linear-in-T coefficient in equation (7), we start from the fact that the phonon drag contribution to the TEP varies from a T^3-like behavior for low T to T^{-1}-like behavior for high T. Since the low T to high T variation of the phonon drag contribution takes place smoothly, we will come across T^2-like, T-like and T^0-like variations while going from the low T side to the high T side. In fact the region near the peak of S may be considered to be a T^0-like (constant) behavior while below that it is a T-like behavior. The T-like portion will get combined with the T-like diffusion contribution. Thus the value of A will be modified from what it would have been in the absence of the phonon drag. For MgB_2 we find $A = 0.04\ \mu$V K^{-2}, while Lorenz *et al* find a slope equal to $0.042\ \mu$V K^{-2}. These slopes are almost equal. In fact, using $W_\pi = 7.4$ eV [8] in equation (4), we find that $W_\sigma \approx 0.57$ eV, which is the same as that obtained by Lorenz *et al* [9]. However, since the phonon drag affects the value of A, it is doubtful to treat the value of W_σ as the value of the (σ-band) Fermi energy. We thus argue that the first term of equation (7) provides only the linear-in-T contribution to the TEP where the diffusion process is modified by the phonon drag process.

We next consider the parameter B. As mentioned above, (the magnitude of) B should vary like θ_D^3. Let θ_{D0} be the Debye temperature of the MgB_2 sample. Then using the values of B from table 1, we can estimate the Debye temperature $\theta_D(x)$ for different x with respect to θ_{D0}. The values of $\theta_D(x)/\theta_{D0}$ obtained in this way are given in the last column of table 1. From these values we see that $\theta_D(x)$ increases with Al content up to $x = 0.4$. Then $\theta_D(x)$ starts to decrease with further increase in x so that for the $x = 0.8$ sample $\theta_D(x)$ takes the lowest value of 0.94 θ_{D0}. For the AlB_2 sample, the Debye temperature is 55% higher than that of the MgB_2 sample. So, in general, Al enhances the Debye temperature of the $Mg_{1-x}Al_xB_2$ system, although in a non-monotonic way. The Debye temperature depends mainly upon two factors. The first is the interatomic coupling, and the second is the mass of the constituent atoms. While $\theta_D(x)$ increases with the interatomic coupling, it decreases with the atomic mass. Since Al is heavier than Mg, we expect a decrease in $\theta_D(x)$ due to the mass effect of Al. But table 1 shows that $\theta_D(x)$ increases with Al content. So we may say that the doping of Al enhances the interatomic coupling in $Mg_{1-x}Al_xB_2$. As the lattice parameters a and c are found to be decrease with Al, the atoms become closer with Al doping. This may be a possible reason for the enhancement of interatomic coupling in the samples considered. It is surprising that the Debye temperature of the $x = 0.8$ sample is lower than θ_{D0}. From figure 2 we see that the resistivity of this sample has

much higher slope values at different T than the other Al doped samples. This means that the situation for the $x = 0.8$ sample is different, which is reflected in the observed TEP also.

As mentioned above, the parameter D also depends on θ_D, like θ_D^2. However, D is expected to involve the effect of varying features of the σ-band also with Al doping. In fact, if D were to depend on θ_D only, the factor $p = |D|\theta_{D0}^2/\theta_D^2$ would have been independent of x. Let us see what actually happens. From table 1 we find that $p = 2.16$, 1.73, 1.33 and 1.53 in units of 10^4 K^3 μV^{-1} for $x = 0.0$, 0.1, 0.2 and 0.4 respectively. Since p is not constant but varies significantly with x, we may say that there is a variation in the σ-band structure due to Al doping, and that the variation has affected the TEP behavior for different Al contents.

4. Conclusions

In this paper, we have presented measurements of the thermoelectric power of the $Mg_{1-x}Al_xB_2$ system for different values of x ranging from zero to one. Measurements of the XRD, magnetization and resistivity are also presented. The thermoelectric power of the $x \leqslant 0.4$ samples vanishes discontinuously below a certain temperature, implying the existence of superconductivity. The thermoelectric power of the $x \geqslant 0.6$ samples is negative, and does not vanish below a finite temperature. This is argued to show that thermoelectric power does not indicate a superconducting effect in the $x \geqslant 0.6$ samples. Another important feature of the thermoelectric power is that its magnitude, $|S|$, starts to increase with temperature, and continues thus up to a certain temperature. The temperature at which $|S|$ is maximum decreases in general with x, going to as low as $T \approx 80$ K for the $x = 0.8$ sample.

In order to explain the observed behavior of the thermoelectric power, we have used a two-band model wherein one band is the 3D π-band and the other one is the 2D σ-band. We have considered both the diffusion process and the phonon drag process to arrive at an interpolation formula from the low T behavior of the diffusion and phonon drag process and the high T behavior of the phonon drag process. The interpolation formula provides an excellent agreement especially for the $x \leqslant 0.6$ samples. For the $x = 0.8$ and 1.0 samples, there is some quantitative disagreement, but the qualitative behavior remains very well matched. We have found that the slope of S with respect to T for the $x = 0$ sample is almost equal to that of the Lorenz *et al* [9] sample.

Another important result from the present study is that in general the Al doping enhances the Debye temperature. The thermoelectric power of the AlB_2 sample does not have a sizable straight-line portion towards low temperature, implying practically no diffusion contribution.

Acknowledgments

The authors from NPL would like to thank Dr Vikram Kumar (Director, NPL) for showing keen interest in the present work. One of us (AVN) thanks the Indian National Science Academy (INSA), New Delhi, for a Senior Scientist position. Two of us (MM and LSSC) would also like to thank CSIR for financial support in the form of (by providing JRF with) a fellowship.

References

[1] Bednorz J G and Müller K A 1986 *Z. Phys.* B **64** 189
[2] Nagamatsu J, Nakagawa N, Muranaka T, Zenitani Y and Akimitsu J 2001 *Nature* **410** 63
[3] Kortus J, Mazin I, Belashchenko K D, Antropovz V P and Boycry L L 2001 *Phys. Rev. Lett.* **86** 4656
[4] Budko S L, Laperot J and Petrovic C 2001 *Phys. Rev. Lett.* **86** 1877
[5] Slusky J S, Rogado N, Regan K A, Hayward M A, Khallfah P, He T, Innumaru K, Loureiro S M, Haas M K, Zandbergan H W and Cava R J 2001 *Nature* **410** 343
[6] Leyrovska L and Leyrovski E 1979 *J. Less-Common Met.* **67** 249
[7] Cooper A S, Corenzwit E, Longinotti L D, Matthias B T and Zachariasen W H 1970 *Proc. Natl Acad. Sci.* **67** 313
[8] An J M and Pickett W E 2001 *Phys. Rev. Lett.* **86** 4366
[9] Lorenz B, Meng R L, Xue Y Y and Chu C W 2001 *Phys. Rev.* B **64** 052513
[10] Mudgel M, Awana V P S, Kishan H and Bhalla G L 2007 *Physica* C **467** 31
[11] Souma S and Takahashi T 2007 *J. Phys.: Condens. Matter* **19** 355003
[12] Gahtori B, Lal R, Agarwal S K, Kuo Y K, Sivakumar K M, Hsu J K, Lin J Y, Rao A, Chen S K and MacManus-Driscoll J L 2007 *Phys. Rev.* B **75** 184513
[13] Putti M, Ferdeghini C, Monni M, Pallecchi I, Tarantini C, Manfrinetti P, Palenzona A, Daghero D, Gonnelli R S and Stepanov V A 2005 *Phys. Rev.* B **71** 144505
[14] Park M-S, Kim H-J, Kang B and Lee S-I 2005 *Supercond. Sci. Technol.* **18** 183
[15] Blatt F J, Schroeder P A and Foiles C L 1976 *Thermoelectric Power of Metals* (New York: Plenum)
[16] Fukuyama H 1984 *Percolation, Localization and Superconductivity* ed A M Goldmen and S A Wolf (New York: Plenum)
[17] Bailyn M 1960 *Phys. Rev.* **120** 381
[18] Mucha J, Pekala M, Szydlowska J, Gadomski W, Akimitsu J, Fagnard J F, Vanerbemden P, Cloots R and Ausloos M 2003 *Supercond. Sci. Technol.* **16** 1167
[19] Cohn J L, Wolf S A, Selvamanicken V and Salama K 1991 *Phys. Rev. Lett.* **66** 1098
[20] Bailyn M 1967 *Phys. Rev.* **157** 480